ELSEVIER

Journal of Nuclear Materials 245 (1997) 169–178

journal of nuclear materials

Further observations on OCOM MOX fuel: microstructure in the vicinity of the pellet rim and fuel–cladding interaction

C.T. Walker [a,*], W. Goll [b], T. Matsumura [c]

[a] *Commission of the European Communities, Joint Research Centre, Institute for Transuranium Elements, Postfach 2340, 76125 Karlsruhe, Germany*

[b] *Siemens-KWU, Postfach 3220, 91058 Erlangen, Germany*

[c] *Central Research Institute of Electric Power Industry, Iwato Kita 2-chome 11-1, Komae-Shi, Tokyo 201, Japan*

Received 12 November 1996; accepted 31 January 1997

Abstract

The fuel investigated was manufactured by Siemens–KWU and irradiated at low rating in the KWO reactor in Germany. The MOX agglomerates in the cold outer region of the fuel shared several common features with the high burn-up structure at the rim of UO_2 fuel. It is proposed that in both cases the mechanism producing the microstructure change is recrystallisation. Further, it is shown that surface MOX agglomerates do not noticeably retard cladding creepdown although they swell into the gap. The contracting cladding appears able to push the agglomerates back into the fuel. The thickness of the oxide layer on the inner cladding surface increased at points where contact with surface MOX agglomerates had occurred. Despite this, the mean thickness of the oxide did not differ significantly from that found in UO_2 fuel rods of like design. It is judged that the high burn-up structure will form in the UO_2 matrix when the local burn-up there reaches 60 to 80 GWd/tM. Limiting the MOX scrap addition in the UO_2 matrix will delay its formation.

1. Introduction

A number of countries have stockpiles of plutonium from the reprocessing of spent light water reactor (LWR) fuel. One way to reduce these stores of separated plutonium is to mix a few percent of it with UO_2 to form a mixed oxide (MOX) fuel and to burn this in a LWR. So far, the majority of the MOX fuels investigated at the Institute for Transuranium Elements have been produced by the optimised co-milling (OCOM) and the ammonium-uranyl-plutonyl-carbonate (AUPuC) processes developed by Siemens–KWU [1]. The fuel manufactured by these processes has a duplex structure and consists of plutonium rich agglomerates up to 200 μm in size irregularly dispersed in a matrix of natural UO_2 containing a small addition of MOX fuel scrap. It has been found that in response to the high local burn-up (up to 200 GWd/tM and more) the MOX agglomerates become highly porous in the course of irradiation [2,3].

This is the second of two papers reporting the results of detailed post-irradiation examinations of OCOM MOX fuel carried out at the Institute for Transuranium Elements. The first paper examined the effect of fuel inhomogeneity on the percentages of fission gas and caesium released during irradiation [3]. This paper focuses on the microstructure changes that occur in the cold outer region of the fuel during irradiation and is concerned principally with four questions. First, is the transformation of the MOX agglomerate microstructure similar to the microstructure changes seen at the surface of UO_2 fuel at high burn-up and is the same mechanism involved? Second, does the swelling of the MOX agglomerates at the pellet rim hinder cladding creepdown and increase fuel–cladding mechanical interaction? Third, do the MOX agglomerates increase the oxidation rate of the cladding and if so is the oxide layer on the cladding inner surface in MOX fuel rods significantly thicker than in UO_2 fuel rods? Finally, since the burn-up in MOX fuel is concen-

* Corresponding author. Tel.: +49-7247 951 477; fax: +49-7247 951 590.

0022-3115/97/$17.00 Copyright © 1997 Elsevier Science B.V. All rights reserved.
PII S0022-3115(97)00009-3

trated in the Pu-rich agglomerates, does the high burn-up structure (rim effect) in the UO_2 matrix form at a higher pellet burn-up than in UO_2 fuel?

Most of the results in the paper are from the same segments of OCOM 15 and OCOM 30 MOX fuel previously used in the investigation of the effects of fuel inhomgeneity on the level of fission gas and caesium release [3].

2. Fuel characteristics and irradiation history

The design characteristics of OCOM MOX fuels manufactured by Siemens–KWU are given in Table 1. It is seen that the fuel contains about 4.5 wt% plutonium of which about 70% is fissile. A small part of this plutonium is recycled material from MOX fuel pellet fabrication (rejected pellets and grinding swarf). Generally this constitutes 5–10% of the total weight of the fuel. As a result of the addition of MOX fuel scrap about 0.2 wt% plutonium is present in the UO_2 matrix before irradiation.

The OCOM 15 fuel contained 34 vol.% of MOX agglomerates with a nominal PuO_2 concentration of 15 wt%, whereas the OCOM 30 fuel contained 17 vol.% of MOX agglomerates with a nominal PuO_2 concentration of 30 wt%. Both segments were irradiated to a burn-up of about 44 GWd/tM under normal PWR conditions in the KWO reactor at Obrigheim in Germany. The irradiation spanned four reactor cycles and lasted 1260 EFPD. During the irradiation, the average linear power was 19.4 kW m^{-1} for the OCOM 15 segment and 20.4 kW m^{-1} for the OCOM 30 segment. In both cases, the linear power during the first reactor cycle was around 16 kW m^{-1} and did not exceed 23 kW m^{-1} in the second, third and fourth cycles. Therefore, the fuel centre temperature was probably barely higher than 1300°C.

The temperature of the cladding outer surface was calculated to be in the range 300–350°C.

Table 1
Fuel pellet and pin segment design characteristics of OCOM MOX fuel manufactured by Siemens–KWU

Fissile Pu [a] (wt%)	3.0
Total Pu (wt%)	4.5
U enrichment (% ^{235}U)	0.72
Grain size [b] (μm)	5–6
Stoichiometry (O/M)	1.995
Fuel density (%TD)	95
Pellet diameter (mm)	9.13
Diameterical gap (mm)	0.17
Fill gas [c]	He (2.25)
Cladding material	Zircaloy-4

[a] $^{239}Pu + {}^{241}Pu$.

[b] Linear intercept.

[c] Figure in parenthesis is the pressure in MPa at room temperature.

3. Temperature distribution in the fuel

In a MOX fuel, most of the heat is generated in the Pu agglomerates. This raises the important question of whether temperature peaks exist at agglomerates which need to be considered in the analysis of MOX fuel behaviour.

From the standard heat conduction equation for a sphere, the maximum temperature difference in the MOX agglomerate, $\Delta\vartheta$, is obtained as

$$\Delta\vartheta_{\text{sphere}}^{\max} = \frac{q''' r_{\text{Pu}}^2}{6\lambda}, \tag{1}$$

where λ is the thermal conductivity, q''', is the power density and r_{Pu} is the radius of the agglomerate. For the evaluation of Eq. (1) conservative values have been used. The average power density in a highly rated MOX fuel (linear rating, $q' = 30$ kW m^{-1} and fuel radius, $r_{\text{fuel}} = 5 \times 10^{-3}$ m) is

$$q'''_{\text{av.}} = \frac{q'}{\pi r_{\text{fuel}}^2} \approx 5 \times 10^8 \text{ W m}^{-3}. \tag{2}$$

Assuming, however, that power is generated only in the MOX agglomerates (volume fraction 0.17) and that the local power density there is three times higher than the average value for the fuel (5×10^8 Wm^{-3}), the maximum power density in a Pu agglomerate, q'''_{agglom} would be about be 9×10^9 Wm^{-3}. Substituting this value in Eq. (1) and using the measured value of the MOX agglomerate radius, $\approx (25 \pm 10)$ μm, and a value of 2.5 Wm^{-1} K^{-1} for the thermal conductivity, λ, the maximum temperature difference between a MOX agglomerate and the surrounding UO_2 matrix, $\Delta\vartheta_{\text{sphere}}^{\max}$, is found to be 0.4°C. Even when less favourable assumptions are made (100 μm agglomerates, and a power density that is four times higher than $q'_{\text{av.}}$) the temperature difference in a Pu agglomerate does not exceed 2°C. The low value can be explained by the smallness of the agglomerates.

4. Methods

The EPMA of xenon, caesium, neodymium and plutonium in the MOX agglomerates and the UO_2 matrix was carried out as described in our previous paper on MOX fuel [3]. The composition of oxide material in the fuel–cladding gap was analysed at 10 kV and 100 nA using a Ni–C multilayer diffraction device for the determination of oxygen. The matrix correction was carried out using the QUAD2 program of Farthing et al. [4]. SEM was performed on a JEOL 35C scanning microscope equipped with a shielded secondary electron detector for the examination of nuclear fuel [5]. Quantitative optical image analysis of the MOX agglomerate porosity was carried out using a Quantimet 520. Measurements were made on electron absorption micrographs produced at 400 and 600 × magni-

fication in the electron microprobe. The pores appeared white in the absorbed electron image and the micrographs were enlarged over the video camera optics to give a magnification of 1200 × at the monitor. At this magnification the smallest feature that can be resolved is around 0.2 μm in size.

5. Results

5.1. Microstructure of the MOX agglomerates

Fig. 1 shows the appearance of a MOX agglomerate at $r/r_o = 0.97$ in an OCOM 30 fuel. It is seen that the agglomerate is characterised by dense clusters of small pores a few microns in size. Results for the volume percentage, number and size of the pores in this agglomerate and in two at $r/r_o = 0.76$ and 0.86 are shown Table 2. It is seen that the agglomerate at $r/r_o = 0.97$ was more porous then the ones examined at $r/r_o = 0.86$ and 0.76 because it contained larger pores. The increase in pore size near the pellet surface is attributed to the fact that local burn-up is higher in this region where the radial depression of the thermal neutron flux is small. Also contained in Table 2 are results for an agglomerate at $r/r_o = 0.85$ in a OCOM 15 fuel irradiated to 43.6 GWd/tM. It is seen that pores in this agglomerate were finer than those observed in the OCOM 30 agglomerate at $r/r_o = 0.86$ and that as a result the level of porosity in the agglomerate was also appreciably lower. Undoubtedly, the difference in the pore size reflects the fact that the burn-up reached in the OCOM 30 agglomerate (250 GWd/tM) was almost twice as high as that attained in the OCOM 15 agglomerate (130 GWd/tM) [3].

Not only do pores form in the MOX agglomerates during irradiations, but also the grain structure is transformed. After irradiation, the agglomerates in the outer region of OCOM fuel comprise of grains 1 to 2 μm in size [6,7]. Before irradiation the mean grain size was of the order of 5 μm. In Fig. 2 a MOX agglomerate near the surface of a OCOM fuel pellet with a burn-up of 40 GWd/tM is shown. The small grain size in the agglomerate is clearly visible.

Table 2
Porosity, pore density and mean pore size in MOX agglomerates in OCOM 30 and OCOM 15 fuel with an average burn-up of approximately 44 GWd/tM

Radial position (r/r_o)	Porosity (%)	Pore density (no. per cm^2)	Mean pore size (μm)
OCOM 30 fuel			
0.97	29.7	4.2×10^8	1.5 (0.1)
0.86	21.9	4.4×10^8	1.3 (0.1)
0.76	24.7	4.3×10^8	1.3 (0.1)
OCOM 15 fuel			
0.85	16.0	7.0×10^8	0.9 (0.1)

The standard deviation is given in parentheses.

5.2. Concentrations of retained xenon and caesium in the MOX agglomerates

Xenon and caesium in the MOX agglomerates behave entirely differently. Caesium is almost completely retained in the agglomerate matrix whereas xenon is almost completely released to the pores in the agglomerate [3]. The concentrations of xenon and caesium retained in the MOX agglomerates in the outer region of an OCOM 15 and an OCOM 30 fuel after irradiation are plotted in Fig. 3 as a function of the local neodymium concentration representing the burn-up. It is seen from the figure that the concentration of xenon in the agglomerates was roughly constant at a low level of around 0.3 wt% regardless of the burn-up. In contrast, the caesium concentration increased almost linearly with the neodymium concentration indicating close

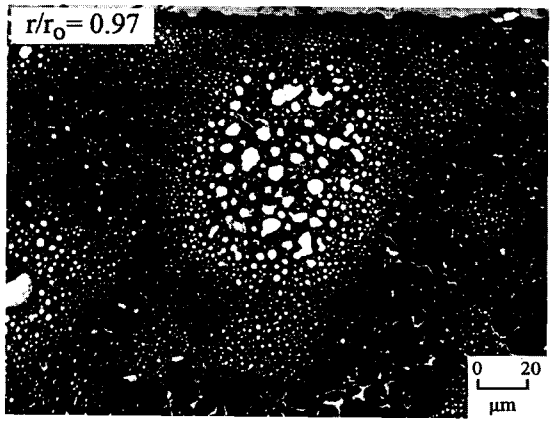

Fig. 1. EPMA electron absorption micrograph showing the appearance of MOX agglomerates at $r/r_o = 0.97$ in an OCOM 30 fuel irradiated to a pellet burn-up of 44.5 GWd/tM (after Walker et al. [3]).

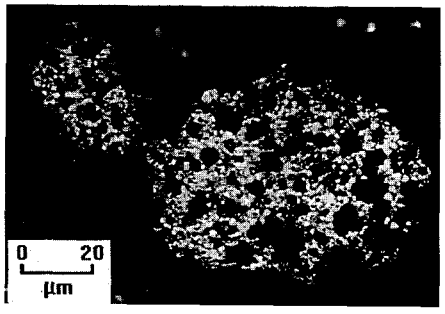

Fig. 2. Optical micrograph showing MOX agglomerates at $r/r_o = 0.99$ near the surface of an OCOM fuel pellet with a burn-up of 40 GWd/tM. The average grain size is around 1.5 μm. Prior to irradiation the grain size was of the order of 5 μm.

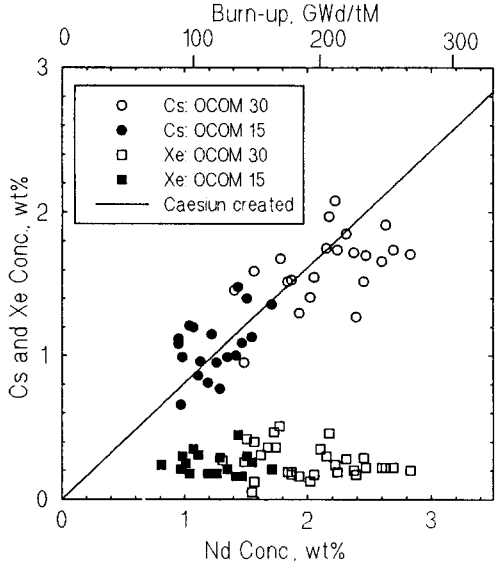

Fig. 3. EPMA results for the concentrations of xenon and caesium in the MOX agglomerates in the outer region of OCOM fuel irradiated to approximately 44 GWd/tM (after Walker et al. [3]). Caesium is almost entirely retained in the MOX agglomerates whereas xenon is almost completely released. The neodymium concentration is a measure of the local burn-up in the agglomerate.

to complete retention by the MOX agglomerates. Only at neodymium concentrations greater than 2.3 wt%, which corresponds to a burn-up of 215 GWd/tM, do the measured caesium concentrations lie consistently below the solid line indicating that some release of caesium occurs.

5.3. Swelling of MOX agglomerates at the fuel surface

The formation of pores causes the MOX aggomerates to swell. Thus agglomerates at the pellet rim tend to expand into the gap in the absence of restraint. The two optical micrographs in Fig. 4 show MOX agglomerates at the surface of fuel pellets with a burn-up of 21.0 and 44.5 GWd/tM. It is seen that at the lower burn-up where fuel–cladding interaction was weak the MOX agglomerate distends into the gap, whereas at the higher burn-up where hard contact occurred it has been pressed into the fuel. Fig. 5 contains data for the growth of surface agglomerates into the gap under conditions of weak fuel–cladding interaction. In the figure the mean height of the MOX agglomerates above the fuel surface is plotted as a function of the pellet burn-up. It is seen that the elevations caused by the agglomerates are less than 10 μm high and that despite weak fuel–cladding interaction increase only slightly with increase in burn-up from about 6 μm at around 20 GWd/tM to about 8 μm at 50 GWd/tM. Data from AUPuC 30 fuel rods are included in the figure. The specifications for the size, volume fraction and plutonium

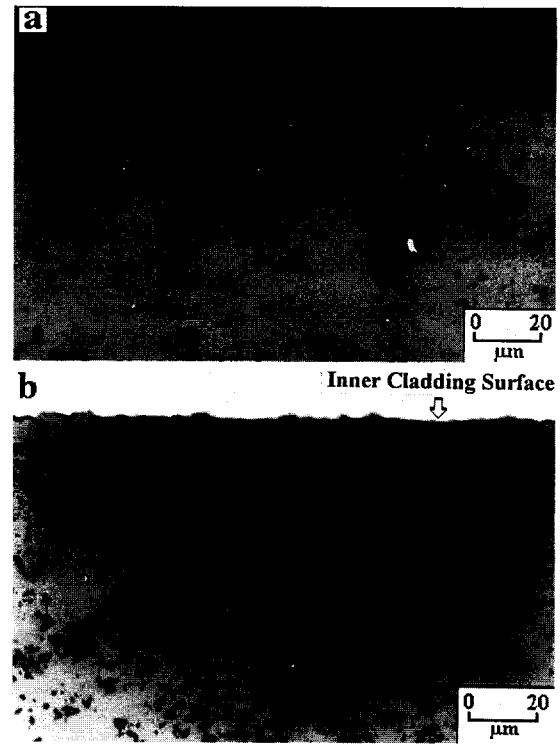

Fig. 4. Optical micrographs showing MOX agglomerates at the surface of OCOM pellets. (a) At a burn-up of 21.0 GWd/tM; (b) at 44.5 GWd/tM. At the lower burn-up the MOX agglomerate distends into the gap, whereas at the higher burn-up it has been pressed into the fuel. In micrograph (a) the inner cladding surface is out of frame.

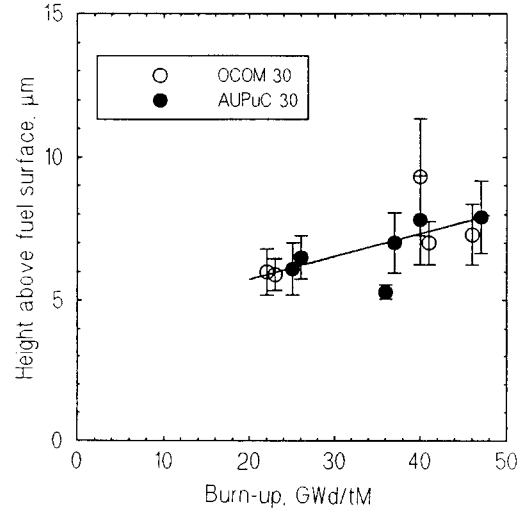

Fig. 5. Growth of surface MOX agglomerates into the gap under conditions of weak fuel–cladding mechanical interaction. The agglomerates begin to distend into the gap at around 20 GWd/tM when the high burn-up structure forms.

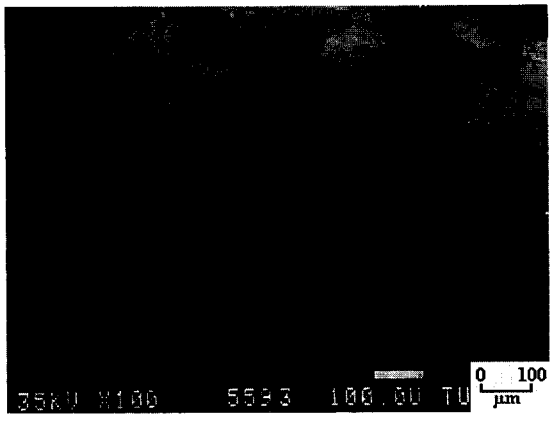

Fig. 6. SEM micrograph showing marks on the cladding inner surface caused by raised MOX agglomerates on the fuel pellet surface. OCOM 30 fuel rod. Pellet burn-up 44.5 GWd/tM.

content of the MOX agglomerates in this fuel are the same as that for the agglomerates in OCOM 30 fuel.

Marks on the cladding inner surface caused by raised MOX agglomerates on the pellet surface are seen in the SEM micrograph in Fig. 6. Each contact point is characterised by light grey island circumscribed by a dark border. Energy dispersive X-ray microanlysis has revealed that the light grey core consists of the outer surface of the agglomerate which has adhered to the cladding surface. The outer dark band is probably a pad of zirconium oxide which originally separated the agglomerate and the cladding wall. This is the result of enhanced oxidation by the MOX agglomerate and because it is thicker than the surrounding zirconium oxide layer it is different in appearance.

5.4. Radial distribution of neodymium and xenon in the UO_2 matrix

Neodymium is a recognised indicator of the local burn-up. This is because it is immobile in UO_2 and mixed oxide fuel and consequently the local concentration of neodymium increases almost linearly with the local burn-up. Further, it has been demonstrated that the xenon level at the pellet surface gives an indication of whether the high burn-up structure has formed [8]. This is because when recrystallisation occurs nearly all the fission gas is swept out of the UO_2 grains. Consequently, the distance over which xenon depletion is measured by EPMA at the pellet surface corresponds to the radial extent of the microstructure transformation.

The radial distributions of neodymium and xenon in the UO_2 matrix in the outer region of an OCOM 30 pellet irradiated to 44.5 GWd/tM are shown in Fig. 7. It is seen that the concentrations of neodymium and xenon increase markedly at the fuel surface. Significantly, for both fission products the increase is steep and continuous. At the pellet rim the concentration of neodymium reached 0.66 wt%

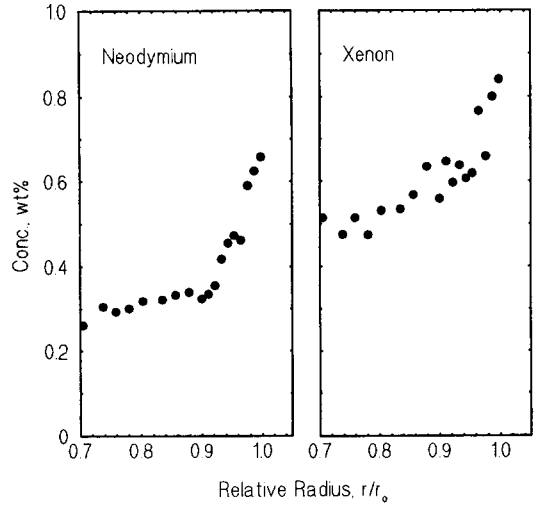

Fig. 7. Radial distribution of neodymium and xenon in the UO_2 matrix in the outer region of an OCOM 30 fuel pellet with a burn-up of 44.5 GWd/tM.

which approximates to a burn-up of 62 GWd/tM and the highest concentration of xenon measured was 0.86 wt%. Taking the fission yield for xenon to be 0.26 the latter concentration also gives a burn-up of 62 GWd/tM indicating that nearly all the fission gas created was retained in the UO_2 lattice.

5.5. Oxide layer on the cladding inner surface

Fig. 8 shows results for the thickness of the oxide layer on the cladding inner surface in OCOM and AUPuC fuel

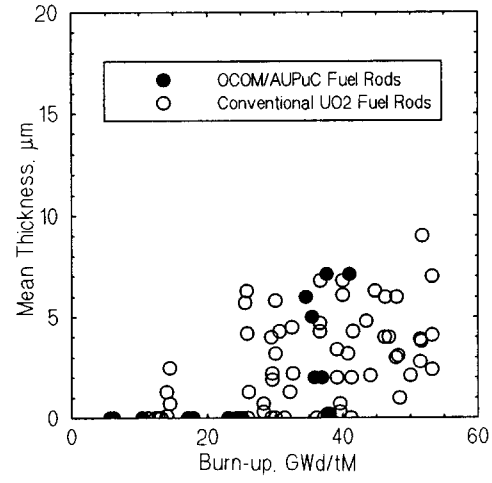

Fig. 8. Thickness of the oxide layer on the cladding inner surface in OCOM and AUPuC fuel rods. Data from conventional UO_2 fuel rods are included for the purposes of comparison. The scatter in the data is due, amongst other things, to a variation in the fuel rating.

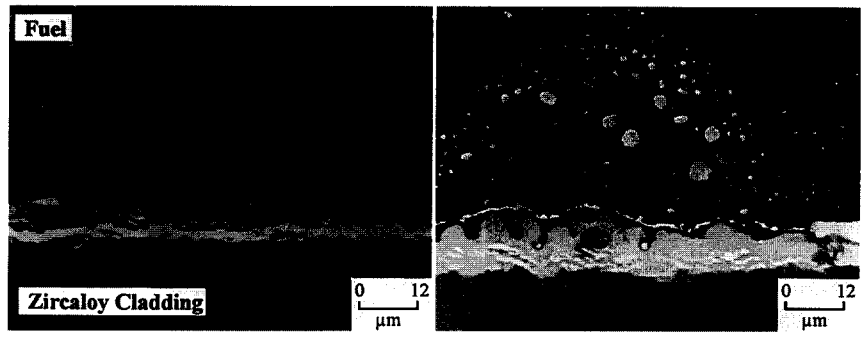

Fig. 9. Electron absorption micrographs showing the two positions where EPMA was carried out on the oxide layer between the fuel and cladding in a OCOM 30 fuel segment. Left, interaction layer contiguous with the UO_2 matix; right, interaction layer at the location of a peripheral MOX agglomerate.

Table 3
Local composition of the oxide layer on the cladding inner surface in an OCOM 30 fuel rod at a pellet burn-up of 44.5 GWd/tM

Location	Concentration wt%								
	Zr	Sn	O	Mo	Ru	Pd	Cs	Xe	Nd
Contiguous with UO_2 matrix	71.2 (0.4)	1.6 (0.1)	25.6 (1.3)	0.4 (0.1)	0.1 (0.1)	0.1 (0.1)	0.3 (0.2)	0.3 (0.1)	0.2 (0.2)
At an agglomerate	70.9 (0.4)	1.5 (0.1)	25.6 (0.8)	0.5 (0.1)	0.1 (0.1)	0.1 (0.1)	0.4 (0.1)	0.5 (0.1)	0.6 (0.2)

Uranium and plutonium were detected at isolated spots suggesting that fuel particles were embedded in the oxide.
The standard deviation is given in parentheses.

rods. For the purposes of comparison, data from conventional UO_2 fuel rods are also included in the figure. It is seen that an oxide layer has not been detected at burn-ups below 25 GWd/tM and that at burn-ups between 35 and 40 GWd/tM the thickness of the oxide layer lies within the range found in conventional UO_2 fuel rods.

The composition of the oxide layer at two azimuthal positions in a section of a OCOM 30 fuel rod with a burn-up of 44.5 GWd/tM has been measured by EPMA. One analysis was made at a position where the UO_2 matrix meets the pellet surface; the other was made at the location of a pheripheral MOX agglomerate. Electron absorption micrographs of the two regions where EPMA was carried out are shown in Fig. 9. It is seen that the oxide layer is noticeably thicker at the location of the agglomerate. Further, at both positions the oxide layer is seen to be firmly attached to the fuel surface, and at the UO_2 matrix there is a distinct end-of life cold gap several microns wide.

EPMA results for the composition of the oxides at the two locations are shown in Table 3. At both the locations analysed the oxide was $Zr_{0.98}Sn_{0.02}O_2$. Where the MOX agglomerate was present at the pellet rim, however, slightly higher concentrations of Mo, Cs, Xe and Nd were measured in the zirconium oxide, although differences generally lie within the limits of uncertainty. The presence of fission products in the oxide is attributed to direct recoil along with weak chemical diffusion.

5.6. Creepdown of the Zircaloy cladding

The maximum diameter change of OCOM fuel rods during irradiation is shown in Fig. 10. Also included in the figure is the range of decrease seen in conventional UO_2 fuel rods. For this OCOM fuel which was irradiated at low power (see Section 2), it is seen that following an initial

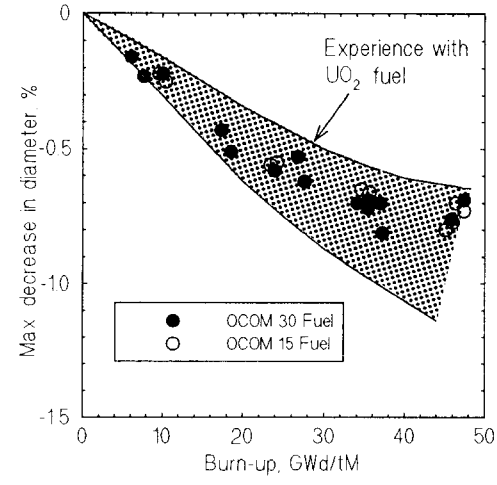

Fig. 10. Diameter decrease of OCOM fuel rods as a function of the burn-up. For the purposes of comparison, the range encountered in conventional UO_2 fuel rods is shown.

decrease at low burn-up, the rod diameter does not change perceptibly with increase in burn-up in the range 30 to 50 GWd/tM. Inspection of the data reveals that the diameter decrease is 0.2 to 0.3% at 10 GWd/tM and 0.7 to 0.8% between 45 and 50 GWd/tM. As indicated in the figure, these diameter changes fall within the range found for UO_2 fuel rods of similar design. The diameter changes measured at high burn-up have been corrected to remove the increase due to the oxide layer on the cladding outer surface.

6. Discussion

6.1. Similarities between the MOX agglomerates and the high burn-up structure at the rim of conventional UO_2 fuel

The MOX agglomerates in the outer low temperature region of OCOM fuel share several common features with the high burn-up structure seen at the rim of conventional UO_2 fuel. As shown in Table 4, the MOX agglomerates and the high burn-up structure both consist of grains and small faceted pores of the order of 1 μm in size. It is also seen that like the high burn-up structure in UO_2 fuel, the agglomerate exhibits strong xenon depletion, with retained concentrations falling to around 0.3 wt%, and almost complete retention of caesium. Although the MOX agglomerates and the high burn-up rim are both porous, it seems that the level of porosity in the agglomerates is substantially higher. This can be explained by the difference in burn-up level. The burn-up in the MOX agglomerates in the OCOM 30 fuel reached about 270 GWd/tM [3], whereas the burn-up at the rim of the UO_2 fuel examined by Spino [9] did not exceed 170 GWd/tM. Thus much more fission gas was formed in the MOX agglomerates which demands increased void space for its accommodation when the microstructure transforms. The SEM micrographs in Fig. 11 show the rim of a UO_2 fuel pellet irradiated to about 45 GWd/tM and an agglomerate in an OCOM MOX fuel. The similarity in microstructure is clearly visible.

Table 4
Similarities between MOX agglomerates and the high burn-up structure at the rim of conventional UO_2 fuel

Characteristic	MOX agglomerate (OCOM 30)	High burn-up structure
Mean grain size (μm)	1.5 ± 0.7 [a]	0.3 ± 0.2 [b]
Porosity (%)	20–30	15–17 [b]
Pore size (μm)	1.3–1.5	1.1–1.2 [b]
Xe retention (wt%)	≤ 0.5	~ 0.25 [c]
Cs retention (wt%)	~ 100	~ 100 [d]

The data for Xe and Cs retention are from EPMA measurements; i.e., they refer not to the concentration retained in the structure as a whole, but in the UO_2 or mixed oxide lattice.
[a] Measured on the agglomerates shown in Fig. 4 at a magnification of 1100X using the linear intercept method.
[b] Spino et al. [9].
[c] Lassmann et al. [8].
[d] Walker et al. [10].

The fact that the MOX agglomerates and the rim of high burn-up UO_2 fuel show distinct similarities is taken as a powerful indication that in both cases the mechanism producing the characteristic microstructure is the same. In agreement with the proposal of Nogita and Une [11] the authors identify this mechanism as recrystallisation induced by the accumulation of irradiation damage and an attendant increase of strain energy in the lattice. If it is accepted that the same mechanism applies, then the finding that larger pores are present in MOX agglomerates close to the fuel surface may provide an insight into the development of structure in UO_2 fuel with increase in burn-up. Moreover, studies of the evolution of the MOX agglomerate microstructure with radial position in the fuel pellet (fuel temperature), such as those already reported by the authors [2,3], could provide clues to how the high burn-up structure in UO_2 fuel evolves with rise in temperature.

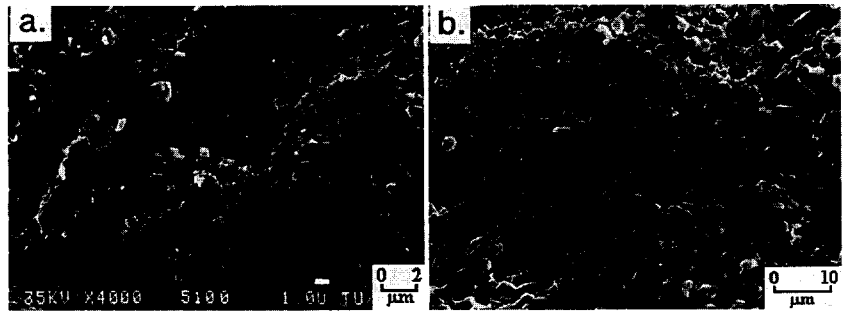

Fig. 11. SEM micrographs showing the high burn-up structure; (a) at the rim of a conventional UO_2 fuel irradiated to 45.2 GWd/tM; (b) in a MOX agglomerate in an AUPuC fuel irradiated to 38.8 GWd/tM. Fine grains and small faceted pores are seen in both micrographs.

It is pointed out that in the OCOM 30 agglomerates the high burn-up structure probably formed at a temperature that was of the order of 100°C higher than that at which it generally forms in high burn-up UO_2 fuel. This is deduced from the fact that the transformation of the fuel microstructure occurs at different stages in the irradiation. In the MOX agglomerates, the high burn-up structure formed at a pellet burn-up of around 20 GWd/tM (approximating to 60 GWd/tM in the agglomerates) when a small gap was present. At the rim of UO_2 fuel, in contrast, it forms at a pellet burn-up of about 45 GWd/tM when the gap is closed. As seen from Table 4, the difference in the temperature of formation does not significantly affect the main characteristics of the structure. This is consistent with an earlier finding [12] that below the temperature for the onset of fuel restructuring and thermally activated fission gas release (1000–1200°C) the appearance of the high burn-up structure does change significantly with radial position in the fuel.

6.2. *Effect of surface MOX agglomerates on cladding creepdown and fuel–cladding mechanical interaction*

The magnitude of cladding creepdown and the level fuel–cladding mechanical interaction in OCOM fuel rods do not appear to be significantly different from that found in conventional UO_2 fuel rods. As seen from Fig. 10, the diameter of OCOM fuel rods decreases by approximately the same amount as UO_2 fuel rods during irradiation. This is principally because OCOM fuel pellets undergo similar dimensional changes to UO_2 fuel pellets [7]. The swelling of surface agglomerates does not significantly alter the fuel pellet diameter. For example, a mean agglomerate height of 7 μm (average maximum) increases the pellet diameter by just 0.15% which as seen from Fig. 10 is of the order of the scatter in the data for the change in the fuel rod diameter. Thus, the surface agglomerates, although they protrude above the fuel surface, cannot retard cladding creepdown significantly. Moreover, when hard fuel–cladding contact occurs, the pressure of the contracting cladding is sufficient to push the agglomerates back into the fuel (see Fig. 4). There appears to be two factors that enable the cladding to do this. First, the agglomerates are more plastic then the surrounding UO_2 matrix because they consist of small recrystallised grains with a low dislocation density. Second, the agglomerate porosity provides ample space for the accomodation of the distended material. During the process in which the agglomerates are squeezed back into the fuel, hard contact with the Zircaloy occurs. As a result of hard contact the surface of the agglomerate becomes embedded in the oxide layer on the inner cladding surface. The bond formed is stronger than the rupture strength of the MOX agglomerates. Hence, when the fuel contracts the surface layer is stripped away (Fig. 6). This probably explains why in Fig. 4(b) a shallow depression appears in the fuel surface at the location of the MOX agglomerates.

6.3. *Effect of MOX agglomerates on oxidation of the cladding inner surface*

Investigation of the oxidation of the inner cladding surface is of interest because it reflects the intensity of the chemical and mechanical interaction between the fuel and the cladding. Generally, a measurable oxide layer is found only after the gap has closed and hard fuel–cladding contact occurs which indicates that solid-state diffusion of oxygen ions into the Zircaloy plays an important role. As a rule of thumb, gap closure in both UO_2 and MOX fuel rods occurs in the burn-up range 20–30 GWd/t and in both significant oxidation of the cladding is first consistently detected at burn-ups above 25 GWd/t (see Fig. 8).

In MOX and AUPuC MOX fuel rods the mean thickness of the Zircaloy oxide layer on the inner cladding surface does not differ significantly from that found in conventional UO_2 fuel rods of similar design (see Fig. 8). There is, however, strong evidence to suggest that the oxide layer is much thicker where MOX agglomerates are located at the fuel surface. For example, it is seen in Fig. 9 that the oxide layer at the MOX agglomerate is almost twice as thick as that next to the UO_2 matrix (i.e., up to 12 μm thick compared with 6 μm). This observation is consistent with the knowledge that because of their high burn-up and because plutonium is the fissile species the MOX agglomerates are more oxidising than the UO_2 matrix. The temperature difference between the MOX agglomerates and the UO_2 matrix does not play an important role, because this is no more than 1 or 2°C (see Section 3).

It is also seen from Fig. 9 that the ZrO_2 layer on the cladding exhibits a corrugated interface with the MOX agglomerates, whereas the the ZrO_2 interface with the UO_2 matrix is relatively smooth. Even the inner ZrO_2-Zircaloy interface opposite the MOX agglomerate shows some corrugation compared to the corresponding interface over from the matrix. Corrugation could be the result of strong fuel–cladding interaction which presses the ZrO_2 layer into surface of the MOX agglomerate. It could also be the result of enhanced inward diffusion of oxygen facilitated by the concentration of rare earth fission products and vacancies in the agglomerates (P.D.W. Bottomley, Institute for Transuranium Elements, personal communication).

6.4. *Formation of the high burn-up structure in the UO_2 matrix at the rim of MOX fuel*

As for conventional UO_2 fuel, it is judged that the high burn-up structure will begin to form in the UO_2 matrix of OCOM fuel once the threshold burn-up is locally exceeded. Lassmann et al. [8] places this in the range 60 to 75 GWd/tM, whereas Kameyama et al. [13] put it in a higher but narrower band of 70 to 80 GWd/tM. Generally,

local burn-ups of these magnitudes are attained at the fuel rim when the pellet burn-up reaches 40–45 GWd/tM. Thus, the burn-ups of both the OCOM 15 and OCOM 30 fuels investigated were within the range at which the high burn-up structure would be expected to begin to form in conventional UO_2 fuel.

From the above it is evident that the magnitude of the local burn-up at the pellet rim determines whether the high burn-up structure forms. This in turn is governed mainly by the amount of fissile material in the UO_2 matrix, which means by the level of uranium enrichment and by the amount of MOX fuel scrap added during fabrication. Although, the addition of scrap containing plutonium is beneficial in the sense that it improves fuel homogeneity, the burn-up in the UO_2 matrix will increase with the quantity of scrap added. This places a ceiling on the amount of MOX scrap that can be added because the presence in the UO_2 matrix of plutonium in concentrations greater than a few wt% will result in the threshold burn-up for the formation of the high burn-up structure being overstepped at the fuel rim.

In the UO_2 matrix of the OCOM 30 fuel the high burn-up structure may have just started to form at some places at the pellet. Evidently, the high burn-up structure was not present where the xenon profile in Fig. 7 was measured, because the xenon concentration increases continuously with the local burn-up. At a second location, however, the fuel microstructure within 50 μm of the pellet surface may just have begun to transform because the concentration of xenon measured fell slightly at the fuel surface. The existence of patches of high burn-up structure around the fuel rim would be consistent with the measured burn-up at the fuel surface of 62 GWd/tM. This burn-up is at the lower end of the range given by Lassmann et al. [8] for the formation of the high burn-up structure in conventional UO_2 fuel.

7. Conclusions

The MOX agglomerates in the outer low temperature region of OCOM fuel share several common features with the high burn-up structure at the rim of conventional UO_2 fuel. These common features include a small grain size, a high density of small faceted pores and strong xenon depletion. Such similarities are taken as a powerful indication that in both cases the mechanism producing the characteristic microstructure is the same. This mechanism is identified as recrystallisation probably induced by the accumulation of irradiation damage and an attendant increase in the strain energy in the lattice.

The magnitude of cladding creepdown and the level of fuel–cladding mechanical interaction in OCOM fuel is not significantly different to that found in conventional UO_2 fuel. Although surface MOX agglomerates protrude into the gap they do not noticeably retard cladding creepdown. First, because OCOM fuel pellets undergo similar dimensional changes to UO_2 fuel pellets. Further, because the swelling of surface agglomerates does not significantly alter the fuel pellet diameter. Moreover, there is evidence that when hard fuel–cladding contact occurs the contracting cladding is able to push the swollen agglomerates back into the fuel.

The mean thickness of the oxide layer on the inner cladding surface in OCOM fuel rods does not differ significantly from that found in conventional UO_2 fuel rods of similar design. Nevertheless, there is strong evidence to suggest that the oxide is thicker at points where contact with surface MOX agglomerates had occurred. Increased oxidation of the Zircaloy cladding takes place at such locations, because the MOX agglomerates, which have a high burn-up, are more oxidising than the surrounding UO_2 matrix. The temperature difference between the MOX agglomerates and the UO_2 matrix does not play an important role, because this is no more than 1 or 2°C

It is judged that the high burn-up structure will begin to form in the UO_2 matrix of OCOM fuel once the threshold burn-up is exceeded. As in conventional UO_2 fuel this will lie in the range 60 to 80 GWd/tM. Accordingly, it is the magnitude of the local burn-up at the pellet rim that determines whether the high burn-up structure forms. This in turn is mainly governed by the amount of fissile material in the UO_2 matrix; that is, by the level of uranium enrichment and by the amount of MOX fuel scrap added during pellet production. In conventional UO_2 fuel, a local burn-up of around 60 GWd/tM is normally obtained at the fuel rim when the pellet burn-up reaches about 45 GWd/tM. Limiting the MOX scrap addition will delay the formation of the high burn-up structure.

Acknowledgements

The paper contains results obtained under contract for Siemens–KWU (Germany) at the Institute for Transuranium Elements (ITU). The authors would like to thank them for permission to publish the results and to acknowledge the contributions of Jose Spino and Enricho Toscano (both of ITU) who obtained some of the data reported. Special thanks are also due to Kees Vennix for his careful and detailed analysis of the porosity in the MOX agglomerates of the OCOM 15 and OCOM 30 fuels and to Klaus Lassmann (ITU) for performing the temperature calculation reported in Section 3.

References

[1] H. Roepenack, F.U. Schlemmer, G.J. Schlosser, Nucl. Technol. 77 (1987) 175.
[2] C.T. Walker, M. Coquerelle, W. Goll, R. Manzel, Nucl. Eng. Des. 131 (1991) 1.

[3] C.T. Walker, W. Goll, T. Matsumura, J. Nucl. Mater. 228 (1996) 8.
[4] I. Farthing, G. Love, V.D. Scott, C.T. Walker, Mikrochim. Acta Suppl. 12 (1992) 117.
[5] M. Coquerelle, P. Knappik, J.-C. Perrier, J. Phys. (Paris) 45 (C2) (1984) 84.
[6] C.T. Walker, M. Coquerelle, in: Proc. Int. Topical Meeting on LWR Fuel Performance: Fuel for the 90's, Vol. 2, Avignon, France, 1991 (ANS/ENS, 1991) p. 506.
[7] W. Goll, H.-P. Fuchs, R. Manzel, F.U. Schlemmer, Nucl. Technol. 102 (1993) 29.
[8] K. Lassmann, C.T. Walker, J. van de Laar, F. Lindström, J. Nucl. Mater. 226 (1995) 1.
[9] J. Spino, C. Vennix, M. Coquerelle, J. Nucl. Mater. 231 (1996) 179.
[10] C.T. Walker, C. Bagger, M. Mogensen, J. Nucl. Mater. 240 (1996) 32.
[11] K. Nogita, K. Une, J. Nucl. Mater. 226 (1995) 302.
[12] C.T. Walker, T. Kameyama, S. Kitajima, M. Kinoshita, J. Nucl. Mater. 188 (1992) 73.
[13] T. Kameyama, T. Matsumura, M. Kinoshita, in: Proc. Int. Topical Meeting on LWR Fuel Performance: Fuel for the 90's, Vol. 2, Avignon, France, 1991 (ANS/ENS, 1991) p. 620.